RESEARCH ARTICLE | DECEMBER 17 2024

A study on martensitic transformation behavior in shape memory alloys via a modulated differential scanning calorimetry technique

Siyao Ma ; Xuexi Zhang ; Guangping Zheng ; Mingfang Qian ; Lin Geng

Appl. Phys. Lett. 125, 252202 (2024)
https://doi.org/10.1063/5.0240749

Applied Physics Letters ARTICLE pubs.aip.org/aip/apl

A study on martensitic transformation behavior in shape memory alloys via a modulated differential scanning calorimetry technique

Cite as: Appl. Phys. Lett. **125**, 252202 (2024); doi: 10.1063/5.0240749
Submitted: 26 September 2024 · Accepted: 6 December 2024 ·
Published Online: 17 December 2024

Siyao Ma,[1,2] Xuexi Zhang,[1,a)] Guangping Zheng,[2,a)] Mingfang Qian,[1] and Lin Geng[1]

AFFILIATIONS

[1]School of Materials Science and Engineering, Harbin Institute of Technology, Harbin 150001, China
[2]Department of Mechanical Engineering, The Hong Kong Polytechnic University, Hong Kong, China

[a)]Authors to whom correspondence should be addressed: xxzhang@hit.edu.cn and mmzheng@polyu.edu.hk

ABSTRACT

Highly precise and efficient characterization of thermophysical parameters associated with martensitic transformation (MT) in shape memory alloys (SMA) is challenging based on conventional calorimetry methods. Moreover, existing methods for evaluating the elastocaloric effect of SMA typically require a series of tests and calculations. In addition, the present method cannot evaluate the nonreversible part during MT. This work proposed a technique rarely mentioned in previous studies on martensitic transformation of metals and alloys, i.e., utilizing the modulated differential scanning calorimetry (MDSC) to superimpose a sinusoidal signal over an underlying DSC ramp. By adjusting appropriate measurement parameters, the reversible and nonreversible parts of thermal events during MT of SMAs were revealed. Furthermore, a series of thermal parameters useful for the study of MT can be obtained by this method and thus may provide a perspective for studying the MT process. Based on MDSC technique, we took Ni-Mn-Sn-(Cu) alloys, a kind of ferromagnetic shape memory alloy, as an example to demonstrate the study of the MT process as well as the elastocaloric effect. From the perspective of energy dissipation, we analyzed the intrinsic relationship between nonreversible component and thermal hysteresis in the MT process. Conventional DSC test and experimental results on the adiabatic temperature change (ΔT_{ad}) were also provided to verify the MDSC prediction results.

Extensive research on thermodynamic analysis of martensitic transformation (MT) has been extensively carried out in the past decades.[1–3] In Ortin and Planes' work,[4,5] they proposed two main driving forces for MT: (1) the chemical driving force, represented by the difference between Gibbs free energy of the two crystalline structures, and (2) non-chemical driving force, i.e., the strain energy generated by the change in the volume of the two phases during MT. The thermal-related signal recorded during the calorimetric tests originated from combination of these two energies. That is to say, conventional calorimetric test, such as differential scanning calorimetry (DSC), can only measure the sum of both thermal events, making it impossible to distinguish the reversible (strain energy part) and nonreversible (Gibbs free energy part) transitions.

The reversible transition of a shape memory alloy (SMA) is related to various functional properties such as vibration damping, actuation, superelasticity, and elastocaloric effect (eCE). On the other hand, the nonreversible transition feature, originated from frictional work dissipation, is very important in SMAs because these materials have to be subjected to millions of cycles with functional property decay. So, it is important to develop a feasible method to evaluate the reversible MT and related properties, such as eCE, which helps in overcoming the time-consuming characterization of eCE.[6–9] In this regard, modulated differential scanning calorimetry (MDSC) appears to be an effective method for this study. MDSC uses two ramp rates simultaneously for thermal analysis, i.e., a linear ramp rate used in a conventional DSC and a periodically varying sinusoidal ramp rate (inset of Fig. 1). The measured heat flow is the total of all the thermal responses. The total heat flow (H) can be divided into a part related to heat capacity (C_p) and that related to the nonreversible heat flow,

$$\frac{dH}{dt} = C_P \frac{dT}{dt} + f(T,t), \tag{1}$$

where dH/dt is the total heat flow under a linear heating rate, C_p is the heat capacity, and dT/dt is the heating rate. The heat flow resulting from the C_p change or heating rate is related to the reversible heat flow. $f(T, t)$ (where T is the absolute temperature and t time) represents

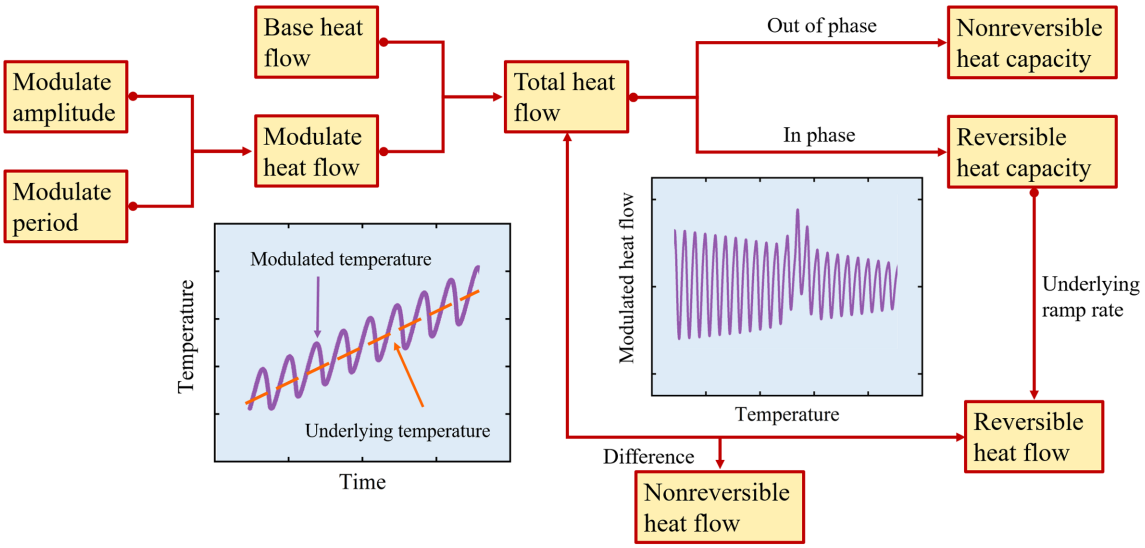

FIG. 1. Scheme of modulated differential scanning calorimetry (MDSC). The left inset shows the modulated temperature change as a function of time, while the right one displays modulated heat flow as a function of temperature.

the nonreversible heat flow and is associated with the kinetics of heat transfer. With MDSC, the heat flow patterns can be resolved into two parts. It is also possible to calculate directly the heat capacity of a sample with the MDSC analysis,

$$C_p = \frac{K_{C_p} A_{M-HF}}{A_{M-HR}}, \tag{2}$$

where $A_{M\text{-}HF}$ is the amplitude of modulated heat flow, $A_{M\text{-}HR}$ is the amplitude of modulated heating rate, and K_{Cp} is C_p calibration constant. It is possible to resolve the contribution of reversible and nonreversible heat flow by superposing the temperature-modulated signals. A pictorial representation of the signals by MDSC technique is given in Fig. 1.

In this work, MDSC, a rarely mentioned technique in martensitic transformation in metals and alloys, was used to investigate the thermodynamic parameters of a Ni-Mn-Sn-(Cu) alloy. At the same time, the intrinsic relationship between the nonreversible component and thermal hysteresis was analyzed. In our research on Ni-Mn-based alloys over the past decade,[10–21] we have found that Ni-Mn-Sn-(Cu) alloys have great potential for development because of their advantages such as its low-cost nontoxic elements and good mechanical properties.[22] In depth study of the thermodynamics of Ni-Mn-Sn-(Cu) alloys is helpful for understanding and effectively regulating its caloric effects. Therefore, the intrinsic relationship between the nonreversible component and thermal hysteresis was analyzed. In addition, the adiabatic temperature change (ΔT_{ad}) of eCE was predicted and compared with that of the experimental tested result. These results demonstrated that MDSC may act as a promising tool for the analysis of MT and may pave a feasible way for the development of advanced caloric materials via an efficient and cost-effective way.

$Ni_{50-x}Mn_{38}Sn_{12}Cu_x$ (x = 0, 2, 3, 4 and 5, hereafter denoted as Cu-x) ingots were prepared by vacuum induction melting under argon atmosphere and cast into a copper mold. Considering the high volatility of Mn in comparison with other used elements, an extra 2 wt. % of Mn was added to make up for the Mn loss during melting. Then, the ingots were sealed in an evacuated quartz tube, annealed at 1173 K for 24 h and quenched in water for compositional homogenization.

The thermal analysis experiments were carried out in a differential scanning calorimeter (DSC, TA Q200) under helium atmosphere, which was operated with either modulated or conventional DSC heating or cooling scans. Using a reference sample of high-purity indium, the calorimeter was calibrated for cell constant, baseline slope, and temperature reading. C_p was calibrated utilizing a standard sample of sapphire using the same experimental conditions at the target temperature. Since MDSC is sensitive to sample size and surface condition, the test samples of $\Phi 2 \times 0.7\,mm^3$ were used.

The modulation heat flow period and heating/cooling rate need to be coordinated to ensure an appropriate number of oscillation cycles in the MT temperature range. After analyzing the parameters selected in the research of polymer materials in the literature[23–30] and conducting multiple attempts in the present work, it was found that ensuring 1–6 cycles of oscillation within the transition temperature range of the tested material is a reasonable parameter. The selection of amplitude requires comprehensive reference to the latent heat and the temperature range for the martensitic transformation obtained from traditional DSC. When the latent heat of phase transition of the tested material is relatively small (less than $5\,J{\cdot}g^{-1}$), a larger modulation amplitude (about 3–10 K) is required. If the temperature range for the martensitic transformation is small (about 3–5 K), a smaller modulation amplitude (0.3–3 K) is required. So, the heating/cooling rate is selected as 5 K/min, and the modulation period can be changed from 40 to 120 s. The modulation amplitude is selected as 5 K. The starting and finishing temperatures of MT were determined via the double tangent method.

The direct measurement of ΔT_{ad} was carried out by a compressive test performed on a universal test machine (Instron-5966) using samples with size of $\Phi 3 \times 4.5\,mm^3$. A maximum stress of 500 MPa was applied during the compressive test. The strain rate during loading and unloading was $3.3 \times 10^{-2}\,s^{-1}$ to reach the adiabatic state. To fully

reflect the elastocaloric effect of the alloys, the test temperature is set to be $A_f + 3$ K for each alloy studied. ΔT_{ad} was monitored using a K-type thermocouple attached to the surface of the sample and was recorded by an OM-DAQ-USB-2401 data acquisition module.

During a DSC test, the temperature changes linearly at a constant heat or cooling rate. However, in the MDSC test, the temperature sinusoidal modulation may overlap on the linear temperature ramp. Therefore, it can be used to differentiate the exothermic and endothermic processes involved during MT. Figure 2 shows the reversible, nonreversible, and total heat flow of a $Ni_{47}Mn_{38}Sn_{12}Cu_3$ alloy obtained at various modulation periods. As shown in Fig. 2(a), when the modulation period is 40 s, the direction of the reversible heat-flow peak is opposite to that of the total heat flow. That indicated that the reversible heat flow is an endothermic process when the total heat flow exhibits an exothermic process. When the modulation period is extended to 60 s [see Fig. 2(b)], the reversible heat flow successively exhibited both exothermic and endothermic peaks. When the modulation period is increased to more than 80 s [as shown in Figs. 2(c) and 2(e)], the reversible heat flow and the total heat flow always have peaks in the same direction.

It is noticed that the modulation period did not affect the nonreversible heat flow peaks, which always followed the direction of the

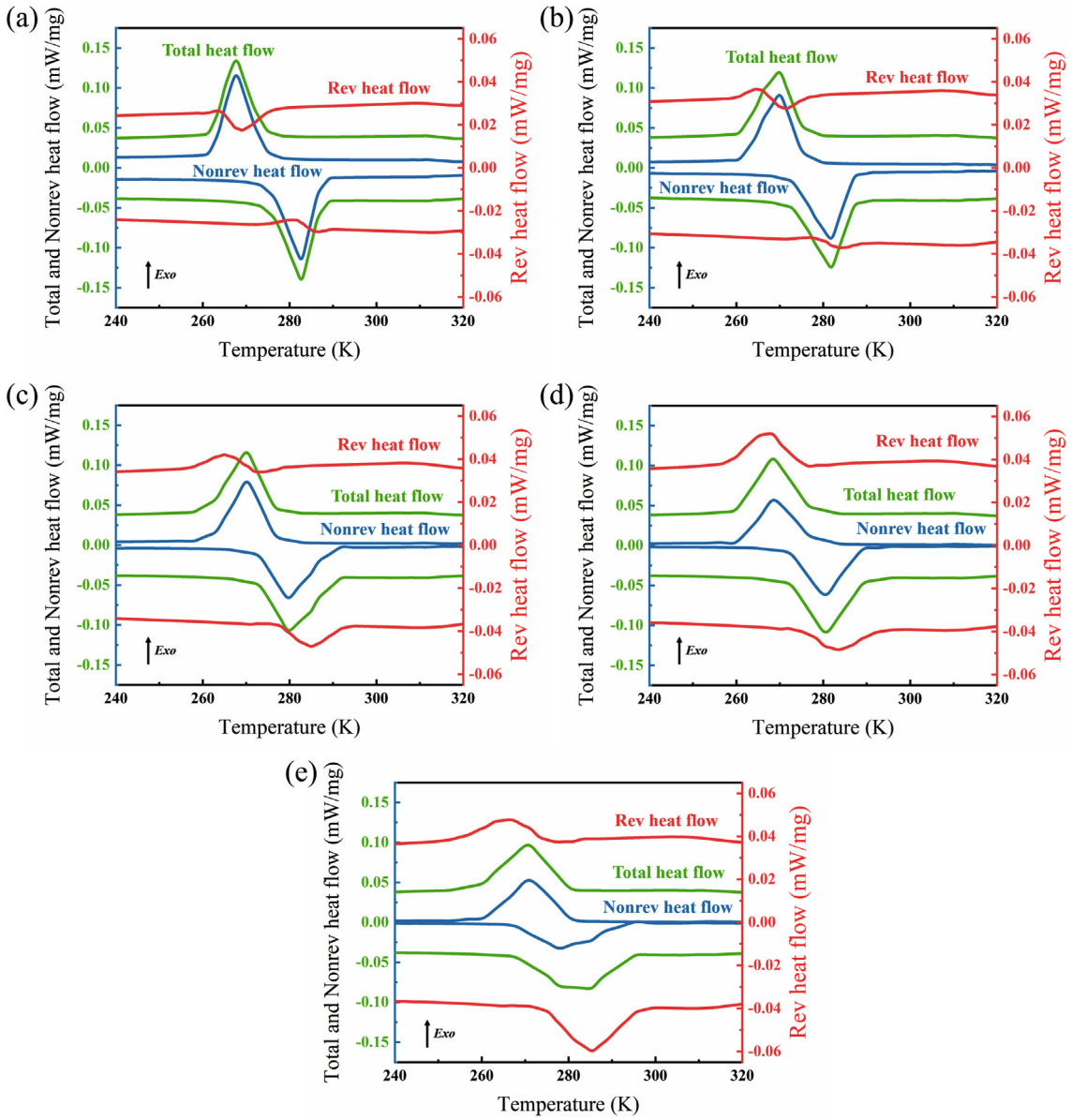

FIG. 2. Reversible, nonreversible, and total heat flow tested using a $Ni_{47}Mn_{38}Sn_{12}Cu_3$ alloy at various modulation periods: (a) 40 s, (b) 60 s, (c) 80 s, (d) 100 s, and (e) 120 s.

TABLE I. MT temperatures (A_f, A_s, M_s, and M_f) by DSC measurements and M-T curves,[21] latent heat of forward and reverse transitions (Q_A and Q_M), frictional work dissipation (E_{fr}), and thermal hysteresis (ΔT_{hys}) of Cu-x alloys.

Cu content x (at. %)	A_f DSC (K)	A_f M-T (K)[21]	A_s DSC (K)	A_s M-T (K)[21]	M_s DSC (K)	M_s M-T (K)[21]	M_f DSC (K)	M_f M-T (K)[21]	Q_A ($J\cdot g^{-1}$)	Q_M ($J\cdot g^{-1}$)	E_{fr} ($J\cdot g^{-1}$)	ΔT_{hys} DSC (K)
0	352	···	340	···	328	···	315	···	9.094	9.472	0.722	24.5
2	315	312	305	302	295	293	286	283	8.566	8.616	0.57	19.5
3	294	282	285	275	277	268	266	255	8.064	8.345	0.549	18
4	274	273	262	266	253	262	241	250	7.045	7.309	0.606	21
5	240	241	227	228	221	220	206	207	5.334	5.647	0.577	20

total heat flow. This is often related to the inevitable occurrence of defects in the crystal, which induced stored elastic strain (ΔH_{el}^{P-M}) at the phase interface between parent and martensite phases. In addition, the energy dissipation in friction (E_{fr}^{P-M}) during interface movement is often heterogeneous. As a result, different martensitic plates or different parts of the same martensitic plate may exhibit different thermal hysteresis. For example, in the cooling process shown in Fig. 2(a), a transition from austenite to martensite occurred under the temperature disturbance (ΔT_1). At this point, the modulated heat flow of the MDSC provides a temperature disturbance (ΔT_2) in the heating direction, which triggers a portion of martensite reverting to the parent phase. Since ΔT_1 is always greater than ΔT_2 during the cooling process, the phase transition from martensite to austenite is incomplete.

Therefore, within a given temperature modulation amplitude, a portion of martensite plates exhibit reversible properties, while the remaining exhibit nonreversible properties. The frictional work dissipation and thermal hysteresis during MT can be further analyzed from these nonreversible signals.

As proposed by Planes *et al.*,[31] the heat ($-Q_M$) released during MT can be expressed as

$$-Q_M = -\Delta H_{ch}^{P-M} + \Delta H_{el}^{P-M} + E_{fr}^{P-M}, \tag{3}$$

where $-\Delta H_{ch}^{P-M}$ is the enthalpy change related to the latent heat of the phase transition, ΔH_{el}^{P-M} is the enthalpy change associated with storage elastic strain, and E_{fr}^{P-M} is the energy dissipation in friction during interface movement. In the reverse MT process, the heat (Q_A) released during forward MT can be expressed as

$$Q_A = \Delta H_{ch}^{M-P} + \Delta H_{el}^{M-P} + E_{fr}^{M-P}. \tag{4}$$

For NiMnSn-based magnetic SMAs, it is found that the magnetization curves in the forward and reverse transition processes are approximately parallel,[32,33] indicating that the elastic strain energy stored in the forward MT is approximately equal to that released in the reverse MT. So, the frictional energy (E_{fr}) can be obtained from Eqs. (3) to (4) that

$$E_{fr} = E_{fr}^{P-M} + E_{fr}^{M-P} = Q_A - Q_M + \Delta H_{ch}^{P-M} - \Delta H_{ch}^{M-P}. \tag{5}$$

Assuming that the interface between parent and martensite phases is a single-phase interface during MT, the entropy change $-\Delta H_{ch}^{P-M}$ can be written as

$$\Delta H_{ch}^{P-M} = T_0 \frac{Q_M}{T_M}, \tag{6}$$

$$\Delta H_{ch}^{M-P} = T_0 \frac{Q_A}{T_A}, \tag{7}$$

where T_0 is the thermodynamic equilibrium temperature[34] at which the Gibbs energies of martensite and austenite phases are equal, which can be estimated by the following relation:

$$T_0 = \frac{M_s + A_f}{2}, \tag{8}$$

where M_s and A_f are martensite starting and austenite finishing temperatures, respectively. From the DSC tests, the characteristic MT temperatures and latent heat of the Cu-x alloys were obtained and summarized in Table I. Comparing the values of characteristic phase transition temperatures measured by DSC with those determined from the thermomagnetic curves as measured under an external field of 0.05 T, it can be found that the measurement results of the two methods are basically consistent.[21] Therefore, the frictional work consumed in the Cu-x alloys with different contents x during a MT cycle can be calculated and is also listed in Table I. It is noticed that the thermal hysteresis of the MT [$\Delta T_{hys} = (A_s + A_f - M_s - M_f)/2$] is related to E_{fr}, demonstrating that E_{fr} can be a good measure for the MT processes.

E_{fr} can also be extended to the study of nonreversible C_p. According to the working principle of MDSC, the nonreversible C_p is obtained by the difference between the measured total C_p and reversible C_p.[35] It is found from Fig. 3 that, for Cu-x alloys, the dependence

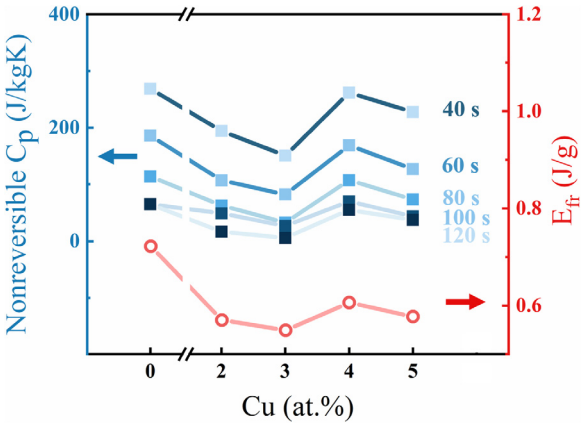

FIG. 3. Nonreversible specific heat capacity (C_p) and frictional work dissipation (E_{fr}) under different modulation periods of Cu-x alloys.

of E_{fr} on x is consistent with the nonreversible specific C_p. The relation between nonreversible C_p and E_{fr} during MT can be established as

$$E_{fr} = C_{p-non}\Delta T_{int}, \tag{9}$$

where ΔT_{int} is the transformation temperature interval [$\Delta T_{int} = (A_f - A_s + M_s - M_f)/2$]. In this way, the nonreversible C_p can be directly characterized by E_{fr}. Although there remain some uncertainties in the interpretation of the data, the reversible and nonreversible signals provide much richer useful information than the conventional DSC.

ΔT_{ad} of eCE can be experimentally monitored using a thermocouple attached to the surface of the samples[8,9] or an infrared camera.[6,7] Here, we propose an indirect way to predict ΔT_{ad} via MDSC technique, which can hardly be realized by conventional DSC.[36,37]

Given that the enthalpy change (Q) of during MT is obtained by integrating the DSC peaks, the temperature change (ΔT_{DSC}) can be estimated by

$$\Delta T_{DSC} = \frac{Q}{C_P}. \tag{10}$$

However, the estimated data (ΔT_{DSC}) are always greater than the actual measured (ΔT_{ad}).[38] This deviation is mainly related to the fact that the Q value obtained from DSC peaks accounts for the reversible and nonreversible parts, in which the former should be used in Eq. (10). The reversible part is related to C_p of the sample, while the nonreversible part is determined by the physical and chemical processes of the sample, which depend on changes in internal variables far from equilibrium but are not driven by the heating rate. Fortunately, the reversible part can be resolved from the MDSC results according to Eq. (1). After the reversible latent heat was resolved, ΔT_{ad} can be accurately estimated using such reversible latent heat and reversible C_p for a SMA.

Here, we take Cu-x alloy as an example to analyze ΔT_{ad} based on the MDSC data. The latent heat of Cu-x alloys under different modulation periods is plotted in Fig. 4. Figure 4(a) shows that the total latent heat of the alloys decreases with increasing Cu content. Such total latent heat is actually the same as those obtained from conventional DSC. The nonreversible latent heat shows a minimum for Cu-3 alloy [Fig. 4(b)], while accordingly the reversible latent heat shows a maximum [Fig. 4(c)].

As Cu-3 alloy exhibits the highest reversible latent heat than that of the other alloys, it should have the highest ΔT_{ad}. Here, ΔT_{ad} was experimentally tested via different techniques and is compared with the calculation results [by Eq. (10)]. The results are shown in Fig. 5.

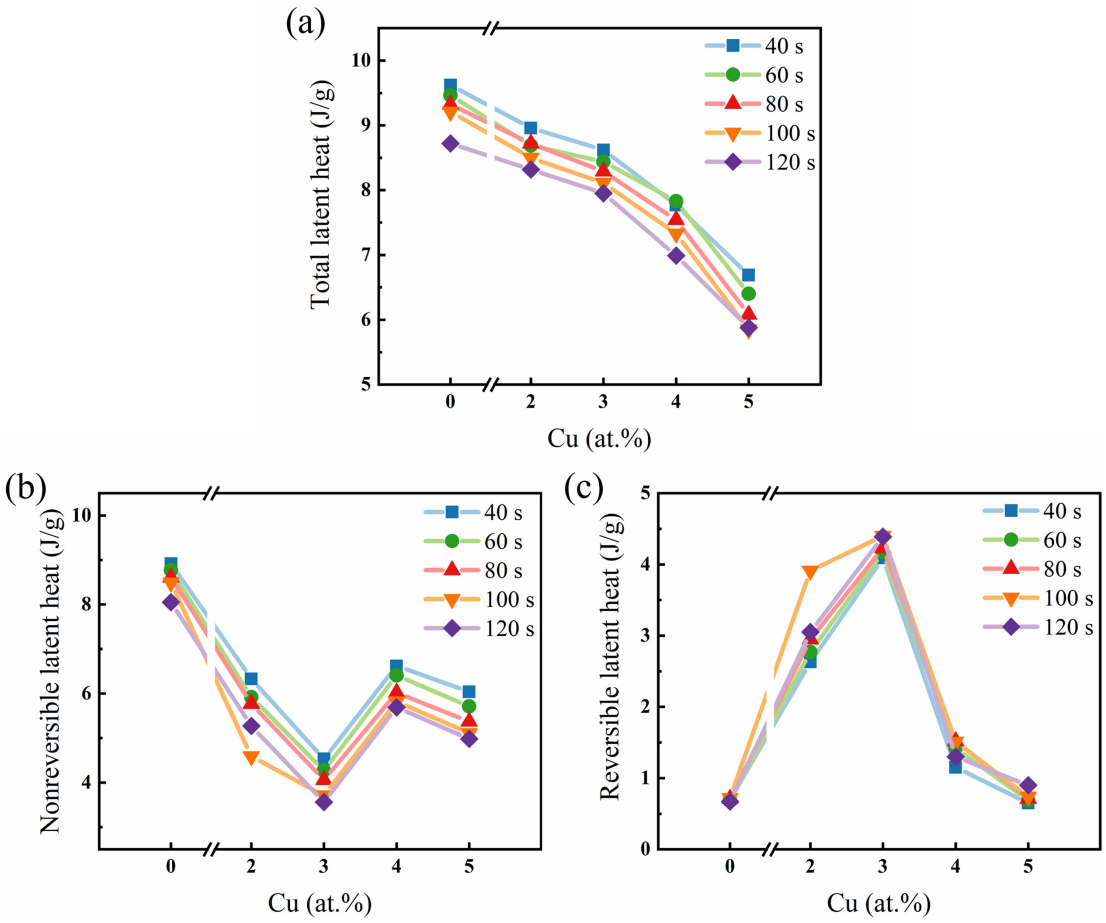

FIG. 4. Latent heat of Cu-x alloys under different modulation periods. (a) Total latent heat, (b) nonreversible latent heat, and (c) reversible latent heat.

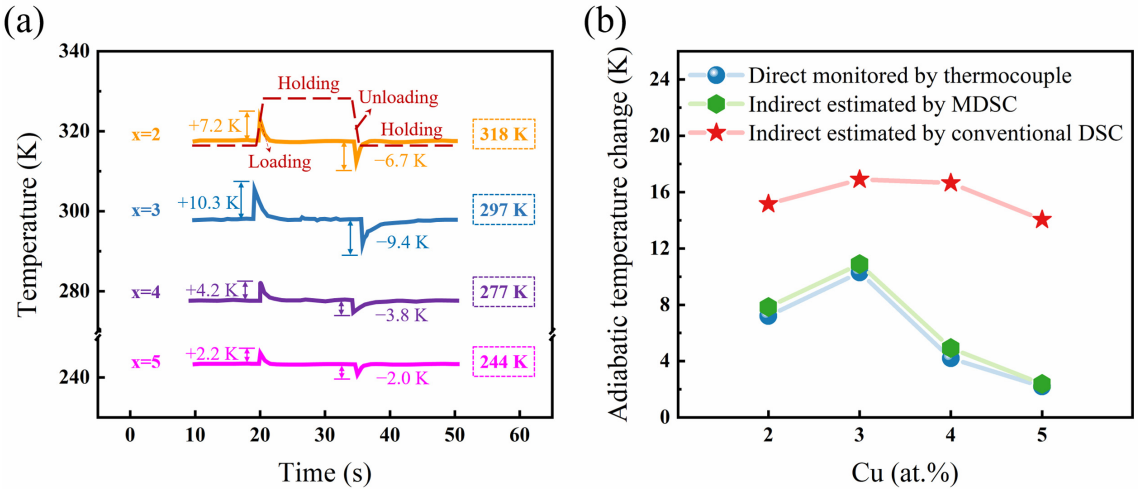

FIG. 5. Experimentally tested and calculated ΔT_{ad} via different techniques in Cu-x alloys. (a) Thermocouple recorded temperature change during loading and unloading process in compressive test and (b) comparison of the experimentally tested and calculated data.

Figure 5(a) shows the direct monitor of ΔT_{ad} for Cu-x alloys during loading and unloading processes under cycling compressive tests (a high-speed loading rate of 3.3×10^{-2} s^{-1} was applied to reach an adiabatic state). The curves show abrupt temperature rise during loading, while a temperature drop upon unloading. The data showed the highest ΔT_{ad} ~10.3 K for the Cu-3 alloy.

The results in Fig. 5(a) and the calculation results based on Figs. 4(a) and 4(c) are summarized in Fig. 5(b). It can be observed in Fig. 5(b) that the estimated ΔT_{ad} obtained from the total latent heat by MDSC (the data are the same as DSC) differs significantly from the directly measured results. In addition, the calculation data based on the reversible latent heat [Fig. 4(c)] are consistent with the experimental results. This confirms that the resolve of the reversible latent heat from MDSC is crucial for the accurate calculation of ΔT_{ad}, demonstrating the reliability of MDSC for the assessment of the eCE. It can also be inferred that the reversible heat flow has a more significant impact on elastocaloric properties in a SMA.

In summary, MDSC is employed to study the evolution of reversible and nonreversible latent heat during MT of Ni-Mn-Sn-(Cu) alloys. The selection method of MDSC measurement parameters was discussed. The thermal parameters, such as latent heat, heat capacity, frictional work dissipation, and thermal hysteresis, were investigated from the MDSC results. The influence of the kinetic component on the MT is investigated by this method, which explains the positive correlation between the frictional work dissipation and the nonreversible heat capacity in Ni-Mn-Sn-(Cu) alloys. Based on the resolved reversible latent heat from MDSC, accurate calculation of the adiabatic temperature change was realized and compared with those of the experimental results. The calculation and experimental results are consistent, demonstrating the reliability of the MDSC for resolve the reversible and nonreversible thermal components of MT and accordingly the fast and reliable analysis of the elastocaloric properties in SMAs.

This work was supported by the National Key R&D program of China (Grant No. 2022YFB3805700) and the National Natural Science Foundation of China (NSFC) (Grant No. 51701052).

AUTHOR DECLARATIONS

Conflict of Interest

The authors have no conflicts to disclose.

Author Contributions

Siyao Ma: Conceptualization (lead); Formal analysis (lead); Investigation (lead); Writing – original draft (lead). **Xuexi Zhang:** Formal analysis (equal); Project administration (equal); Writing – review & editing (equal). **Guangping Zheng:** Formal analysis (equal); Investigation (equal); Writing – review & editing (equal). **Mingfang Qian:** Investigation (equal); Writing – review & editing (equal). **Lin Geng:** Investigation (equal); Project administration (equal).

DATA AVAILABILITY

The data that support the findings of this study are available from the corresponding authors upon reasonable request.

REFERENCES

[1]H. Kato, Y. Yasuda, and K. Sasaki, Acta Mater. **59**(10), 3955–3964 (2011).
[2]S. Belyaev, N. Resnina, E. Demidova, A. Ivanov, A. Shelyakov, V. Andreev, V. Chekanov, and E. Ubyivovk, J. Alloys Compd. **902**, 163570 (2022).
[3]I. Müller and S. Seelecke, Math. Comput. Modell. **34**(12-13), 1307–1355 (2001).
[4]J. Ortín and A. Planes, Acta Metall. **37**(5), 1433–1441 (1989).
[5]J. Ortín and A. Planes, Acta Metall. **36**(8), 1873–1889 (1988).
[6]G. J. Pataky, E. Ertekin, and H. Sehitoglu, Data Brief **5**, 7–8 (2015).
[7]H. Ossmer, F. Lambrecht, M. Gültig, C. Chluba, E. Quandt, and M. Kohl, Acta Mater. **81**, 9–20 (2014).
[8]J. Cui, Y. Wu, J. Muehlbauer, Y. Hwang, R. Radermacher, S. Fackler, M. Wuttig, and I. Takeuchi, Appl. Phys. Lett. **101**(7), 073904 (2012).
[9]Z. Yang, D. Y. Cong, X. M. Sun, Z. H. Nie, and Y. D. Wang, Acta Mater. **127**, 33–42 (2017).
[10]M. Chmielus, X. X. Zhang, C. Witherspoon, D. C. Dunand, and P. Müllner, Nat. Mater. **8**(11), 863–866 (2009).
[11]M. Qian, X. Zhang, L. Wei, P. Martin, J. Sun, L. Geng, T. B. Scott, and H. X. Peng, Sci. Rep. **8**(1), 16574 (2018).

[12]H. Zhang, M. Qian, X. Zhang, L. Wei, F. Cao, D. Xing, X. Cui, J. Sun, and L. Geng, J. Alloys Compd. **689**, 481–488 (2016).
[13]H. Zhang, M. Qian, X. Zhang, S. Jiang, L. Wei, D. Xing, J. Sun, and L. Geng, Mater. Des. **114**, 1–9 (2017).
[14]L. Wei, X. Zhang, M. Qian, X. Cui, L. Geng, J. Sun, L. V. Panina, and H.-X. Peng, Mater. Des. **112**, 339–344 (2016).
[15]L. Wei, X. Zhang, W. Gan, C. Ding, and L. Geng, Scr. Mater. **168**, 28–32 (2019).
[16]X. Zhang, H. Zhang, M. Qian, and L. Geng, Sci. Rep. **8**(1), 8235 (2018).
[17]X. Zhang, M. Qian, S. Miao, R. Su, Y. Liu, L. Geng, and J. Sun, J. Alloys Compd. **656**, 154–158 (2016).
[18]R. Zhang, X. Zhang, M. Qian, J. Sun, and L. Geng, Intermetallics **97**, 1–7 (2018).
[19]H. Zhang, X. Zhang, M. Qian, B. Yuan, and L. Geng, Intermetallics **105**, 124–129 (2019).
[20]R. Zhang, X. Zhang, M. Qian, and L. Geng, Metall. Mater. Trans. A **49**(12), 6416–6425 (2018).
[21]S. Ma, X. Zhang, G. Zheng, M. Qian, and L. Geng, Materials **17**(13), 3172 (2024).
[22]Y. Li, W. Sun, D. Zhao, H. Xu, and J. Liu, Scr. Mater. **130**, 278–282 (2017).
[23]A. Orzeszko and A. Sikorski, Eur. Polym. J. **29**(4), 593–596 (1993).
[24]M. Reading, A. Luget, and R. Wilson, Thermochim. Acta **238**, 295–307 (1994).
[25]G. Van Assche, A. Van Hemelrijck, H. Rahier, and B. V. Mele, Thermochim. Acta **268**, 121–142 (1995).
[26]X. Hu, C. D. Breach, and R. J. Young, Polymer **38**(4), 981–983 (1997).
[27]E. Verdonck, K. Schaap, and L. C. Thomas, Int. J. Pharm. **192**(1), 3–20 (1999).
[28]B. B. Sauer, W. G. Kampert, E. Neal Blanchard, S. A. Threefoot, and B. S. Hsiao, Polymer **41**(3), 1099–1108 (2000).
[29]W. Chen, I.-K. Moon, and B. Wunderlich, Polymer **41**(11), 4119–4125 (2000).
[30]Z. Qiu, T. Ikehara, and T. Nishi, Polymer **44**(10), 3095–3099 (2003).
[31]E. O. A. Planes, A. Gonzàlez-Comas, and L. Mañosa, Phys. Rev. Lett. **79**(20), 3926–3929 (1997).
[32]D. Y. Cong, L. Huang, V. Hardy, D. Bourgault, X. M. Sun, Z. H. Nie, M. G. Wang, Y. Ren, P. Entel, and Y. D. Wang, Acta Mater. **146**, 142–151 (2018).
[33]T. Krenke, E. Duman, M. Acet, E. F. Wassermann, X. Moya, L. Manosa, and A. Planes, Nat. Mater. **4**(6), 450–454 (2005).
[34]H. C. Tong and C. M. Wayman, Acta Metall. **22**(7), 887–896 (1974).
[35]A. Wurm and C. Schick, Colloid Polym. Sci. **281**(2), 113–122 (2003).
[36]E. Stern-Taulats, P. O. Castillo-Villa, L. Mañosa, C. Frontera, S. Pramanick, S. Majumdar, and A. Planes, J. Appl. Phys. **115**(17), 173907 (2014).
[37]X. Moya, E. Stern-Taulats, S. Crossley, D. González-Alonso, S. Kar-Narayan, A. Planes, L. Mañosa, and N. D. Mathur, Adv. Mater. **25**(9), 1360–1365 (2013).
[38]H. Hou, E. Simsek, D. Stasak, N. A. Hasan, S. Qian, R. Ott, J. Cui, and I. Takeuchi, J. Phys. D: Appl. Phys. **50**(40), 404001 (2017).